Nucleotide Dependent Intrinsic Fluorescence Changes of W29 and W36 in Smooth Muscle Myosin

Marilyn van Duffelen, Lynn R. Chrin, and Christopher L. Berger
Department of Molecular Physiology and Biophysics, University of Vermont, College of Medicine, Burlington, Vermont 05405-0068

ABSTRACT The intrinsic fluorescence of smooth muscle myosin is sensitive to both nucleotide binding and hydrolysis. We have examined this relationship by making MDE mutants containing a single tryptophan residue at each of the seven positions found in the wild-type molecule. Previously, we have demonstrated that a conserved tryptophan residue (W512) is a major contributor to nucleotide-dependent changes of intrinsic fluorescence in smooth muscle myosin. In this study, an MDE containing all the endogenous tryptophans except W512 (W512 KO-MDE) decreases in intrinsic fluorescence upon nucleotide binding, demonstrating that the intrinsic fluorescence enhancement of smooth muscle myosin is not solely due to W512. Candidates for the observed quench of intrinsic fluorescence in W512 KO-MDE include W29 and W36. Whereas the intrinsic fluorescence of W36-MDE is only slightly sensitive to nucleotide binding, that of W29-MDE is paradoxically both quenched and blue-shifted upon nucleotide binding. Steady-state and time-resolved experiments suggest that fluorescence intensity changes of W29 involve both excited-state and ground-state quenching mechanisms. These results have important implications for the role of the N-terminal domain (residues 1–76) in smooth muscle myosin in the molecular mechanism of muscle contraction.

INTRODUCTION

Muscle contraction at the molecular level is driven by the cyclic interaction of myosin, a ubiquitous motor protein, and polymeric actin. Interdigitated filaments of myosin (thick filaments) and actin (thin filaments) are arranged in parallel and slide past one another, causing muscle shortening and force production during contraction in striated muscle (Huxley and Hansen, 1954; Huxley and Niedergerke, 1954). Filament sliding is thought to be achieved by structural transitions in the globular regions of myosin, known as cross-bridges, which extend away from the thick filaments and interact with actin in a cyclic manner (Huxley, 1969). Structural transitions in myosin during muscle contraction are believed to be mediated by chemical transitions between intermediate states of the myosin ATPase cycle, which have been well studied by transient presteady-state and steady-state kinetic methods (reviewed by Cooke, 1999; Geeves and Holmes, 1999) and summarized below (Scheme I).

$$\mathrm{M} + \mathrm{ATP} \overset{K_1}{\leftrightarrow} \mathrm{M}^{*} \cdot \mathrm{ATP} \overset{K_2}{\leftrightarrow} \mathrm{M}^{**} \cdot \mathrm{ADP.P}i \overset{K_3}{\leftrightarrow} \mathrm{M}^{*} \cdot \mathrm{ADP} + \mathrm{P}i \overset{K_4}{\leftrightarrow} \mathrm{M} + \mathrm{ADP}$$

SCHEME 1

Of particular importance to the current work is the enhancement of intrinsic tryptophan fluorescence in myosin upon nucleotide binding (*) and hydrolysis of ATP (**), which have been exploited to examine the rates of the reaction steps in skeletal and smooth muscle myosin in both the absence and presence of actin (Lymn and Taylor, 1971; Bagshaw and Trentham, 1974; Bagshaw et al., 1974; Marston and Taylor, 1980; Rosenfeld and Taylor, 1984; Cremo and Geeves, 1998). In this scheme, myosin initially binds ATP, resulting in the first level of intrinsic tryptophan fluorescence enhancement (*). Next, the rapid and reversible hydrolysis of ATP results in an additional enhancement of intrinsic tryptophan fluorescence (**). After hydrolysis, inorganic phosphate and ADP are sequentially released, with an associated decrease in intrinsic tryptophan fluorescence at each step. The phosphate-release step is rate-limiting and shifts myosin from a weak to strong actin binding conformation. It is this step that is believed to be associated with force generation during muscle contraction. The nucleotide-free complex (the ''rigor'' state) remains strongly bound to actin until dissociated by the binding of ATP to start a new contractile cycle. Therefore, although shown in linear form, Scheme 1 describes the cyclic process of nucleotide binding, hydrolysis, and product release by myosin.

The structural basis of these nucleotide-dependent intrinsic fluorescence changes in myosin II has been previously investigated in skeletal muscle (Park et al., 1997), smooth muscle (Yengo et al., 1998, 2000), and the slime-mold *Dictyostelium discoideum* (Batra and Manstein, 1999; Kovács et al., 2002; Málnási-Csizmadia et al., 2000). In all three isoforms, a single tryptophan residue (W501 in *D. discoideum* nonmuscle myosin II, W510 in skeletal muscle myosin, and W512 in smooth muscle myosin) has been shown to be the largest contributor to the observed intrinsic fluorescence enhancement associated with nucleotide binding and/or hydrolysis. This conserved tryptophan is located

Submitted April 13, 2004, and accepted for publication May 14, 2004.

Address reprint requests to Christopher L. Berger, Tel.: 802-656-0832; Fax: 802-656-0747; E-mail: christopher.berger@uvm.edu.

Abbreviations used: DTT, dithiothreitol; ELC, essential light chain; MDE, motor domain essential light chain; MOPS, 3-[*N*-morpholino]propanesulfonic acid; S1, subfragment 1.

© 2004 by the Biophysical Society

0006-3495/04/09/1767/09 $2.00

doi: 10.1529/biophysj.104.044388

in the relay loop, a region of myosin thought to be critically involved in the conduction and amplification of structural changes at myosin's active site to the lever arm and actin-binding interface (reviewed by Houdusse and Sweeney, 2001). W501 has been shown to be the only tryptophan residue to participate in the intrinsic fluorescence enhancement associated with the ATPase cycle in *D. discoideum* nonmuscle myosin II (Batra and Manstein, 1999; Málnási-Csizmadia et al., 2000). The situation has been demonstrated to be more complicated in skeletal muscle myosin, with two tryptophans unique to this isoform (W113 and W131) potentially contributing to the overall enhancement of intrinsic fluorescence as well as W510 (Park and Burghardt, 2000; Kovács et al., 2002). It remains to be shown that W512 is uniquely sensitive to nucleotide binding and hydrolysis in smooth muscle myosin.

In addition to W512's sensitivity to nucleotide, we have previously demonstrated that, although not responsive to nucleotide binding, W546 is sensitive to actin binding (Yengo et al., 1998), whereas tryptophans 441, 597, and 625 are all insensitive to both nucleotide and actin binding (Yengo et al., 2000, 1998).The catalytic motor domain of smooth muscle myosin (Fig. 1) contains seven tryptophan residues (29, 36, 441, 512, 546, 597, and 625). Thus the potential contributions of W29 and W36 to the observed intrinsic fluorescence changes in smooth muscle myosin upon nucleotide binding and hydrolysis are as of yet uncharacterized. In this study, we have generated a W512 knockout construct of smooth muscle myosin (W512 KO-MDE) that contains the six endogenous tryptophans other than W512, which was conservatively mutated to phenylalanine. We also constructed two mutants, W29-MDE and W36-MDE, each of which contains a single endogenous tryptophan at residue 29 or 36, respectively. The W512 KO-MDE demonstrates a small quench in the presence of nucleotide. Therefore, the intrinsic fluorescence enhancement of smooth muscle myosin is not solely due to the conserved tryptophan residue (W512) that resides in the relay loop. Subsequently, we investigated the possible contributions to the intrinsic fluorescence enhancement of smooth muscle myosin by W29 and W36, which have not been examined directly before. Both residues, which reside near the SH3 domain at the N-terminus of the smooth muscle myosin heavy chain and are unique to this isoform, are sensitive to nucleotide binding, albeit less than W512 in the relay loop.

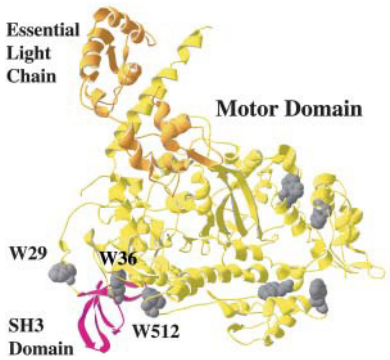

FIGURE 1 Crystal structure of the smooth muscle myosin MDE construct with the myosin heavy chain colored yellow (residues 1–819) and the essential light chain colored orange. The seven endogenous tryptophans are space filled and colored gray, and the N-terminal SH3 domain (residues 33–76) adjacent to W29 and containing W36 is colored pink (Dominguez et al., 1998).

METHODS

Mutagenesis

Generation of the WT-MDE and W512-MDE constructs was previously described (Yengo et al., 2000). The W512 KO-MDE construct, in which W512 was conservatively replaced with phenylalanine, was generated by PCR-mediated site-directed mutagenesis from a cDNA of smooth muscle myosin heavy chain containing the motor domain and essential light chain binding regions (residues 1–819, kindly provided by Kathleen M. Trybus, University of Vermont). We also constructed two mutants containing a single tryptophan, W29-MDE and W36-MDE. Beginning with a Null-MDE construct (Yengo et al., 2000) in which all the endogenous tryptophans had been replaced with phenylalanine or methionine, the W29 was restored to create W29-MDE, or the W36 was restored for the W36-MDE construct. All PCR-amplified construct sequences were confirmed by the University of Vermont DNA Sequencing Facility.

Protein expression and purification

MDE cDNA was cloned into the pVL-1392-NE baculovirus transfer vector (Invitrogen, Carlsbad, CA) containing a FLAG affinity tag (DYKDDDDK), transfected into Sf9 cells with Baculo-Gold (BD Biosciences Pharmingen, Boston, MA), amplified, then expressed and purified on a FLAG affinity column (Sigma, St. Louis, MO) to yields of 1–3 mg per 1×10^9 Sf9 cells. The final product was stored in MDE buffer containing 10 mM MOPS, 20 mM KCl, 1 mM EGTA, 1 mM NaN_3, and 1 mM DTT, pH 7.4, RT.

Functional assays

Actin-activated ATPase rates were determined by an enzyme-linked assay as previously described (Furch et al., 1998; De la Cruz et al., 2000) in a modified ATPase buffer (10 mM MOPS, 25 mM KCl, 2 mM $MgCl_2$, 1 mM EGTA, 1 mM DTT, pH 7.0, 25°C). Purified MDE was assayed at a concentration of 1–4 μM in the presence of 0–120 μM actin. The average actin-activated ATPase rates of the MDE preparation were plotted as a function of actin concentration and fit with a nonlinear least-squares method using OriginLab software (Northampton, MA). Values of V_{max} and K_M were calculated using Michaelis-Menton kinetics.

Fluorescence measurements

Steady-state tryptophan fluorescence measurements were made essentially as described (Yengo et al., 2000) using a Quantamaster fluorometer (Photon Technology International, South Brunswick, NJ) equipped with a 75 or 150 W Xenon arc lamp as an excitation source, excitation/emission monochrometers, and a WG320 cutoff emission filter. Tryptophan emission spectra were measured by exciting the sample at 295 nm and collecting the emitted fluorescence at 305–400 nm. Slit widths were set at a resolution of 1–2 nm for excitation and 4–5 nm for emission. Fluorescence emission

spectra were measured for each of the purified proteins in MDE buffer (10 mM MOPS, 20 mM KCl, 1 mM EGTA, 1 mM NaN_3, 1 mM DTT, pH 7.4, RT) in the presence of saturating amounts of ADP (20–200 μM) or ATP (2 mM) as well as in the absence of nucleotide. All fluorescence spectra were corrected for Raman scatter and background fluorescence.

Acrylamide quenching was used to determine the degree of solvent exposure of W29 and W36 in the presence and absence of 2 mM ATP as previously described (Yengo et al., 2000). The decrease in fluorescence intensity at the emission maximum (λ_{max}) of the steady-state emission spectrum was measured as a function of increasing acrylamide concentrations ([Q]). The fluorescence intensity in the absence of quencher (F_0) divided by the fluorescence intensity in the presence of quencher (F) was used to quantify the relative change in fluorescence from acrylamide quenching (F_0/F). F_0/F was plotted as a function of [Q] and fit to the Stern-Volmer relationship, taking into account both static (V) and dynamic (K_{SV}) quenching constants: $F_0/F = (1 + K_{SV}[Q])(\exp V[Q])$(Eftink and Ghiron, 1976). The static quenching value, which determines the upward curvature of the Stern-Volmer plot, was previously determined to be $V = 3.0\ M^{-1}$ (Yengo et al., 2000). Therefore, the dynamic quenching constant was determined by fitting the Stern-Volmer plots by a nonlinear least squares method using OriginLab software. The bimolecular quenching constant was calculated by normalizing the measured dynamic quenching constant to the observed tryptophan average lifetime ($k_q = K_{sv}/\tau_{avg}$).

Tryptophan lifetime measurements in the presence and absence of 0.2 mM ADP or 2 mM ATP were measured with a Photon Technology International (London, Canada) Laserstrobe system with a nitrogen-pumped dye laser emitting at 590 nm and frequency doubled to 295 nm. Total fluorescence emission was detected through a WG320 cutoff filter using a stroboscopic detection system with a time-delay gated photomultiplier tube. The instrument response function was collected by determining the peak time delay of light scattered at 295 nm by nonfat dry milk solids and used to deconvolute the experimental time-resolved emission decays using proprietary software from Photon Technology International. The data were best fit to a two-exponential decay. The time-resolved quantum yield was calculated relative to the natural tryptophan lifetime (16 ns). Quantum yield and bimolecular quenching constant calculations were made using an amplitude weighted average lifetime value ($\tau_{avg} = (\tau_1 \times ampl_1)/(ampl_1 + ampl_2) + (\tau_2 \times ampl_2)/(ampl_1 + ampl_2)$).

Analysis of protein crystal structures

The three-dimensional structures of smooth muscle myosin MDE in the presence of ADP · AlF_4^- (1BR1.pdb) and ADP · BeF_x (1BR4.pdb) were visualized and analyzed in terms of intramolecular distances and B-factor values in Swiss-PDB Viewer (GalaxoSmithKline, Middlesex, UK). The solvent-accessible surface areas of W29 and W36 were calculated using a script in XPLOR (Molecular Simulations, San Diego, CA), which describes the center of a spherical solvent molecule of radius 1.6 Å rolling along the protein surface.

RESULTS

Functional assays

Actin-activated ATPase assays were used to access the functionality of the expressed MDE constructs. In these assays, the steady-state ATPase rate of each MDE construct at various concentrations of actin (0–120 μM) was followed by stopped flow at 25°C (De la Cruz et al., 2000; Furch et al., 1998). The smooth muscle myosin WT-MDE construct containing the seven endogenous tryptophans is compared to the W512 KO-MDE mutant lacking W512, and the single tryptophan containing W29-MDE and W36-MDE mutants. The Michaelis-Menton constants of WT-MDE, W512 KO-MDE, W29-MDE, and W36-MDE are presented in Table 1. By this assay, these constructs all show enhanced ATPase rates in the presence of actin, with V_{max} values of 0.17 ± 0.09 s^{-1} for WT-MDE, 0.08 ± 0.05 s^{-1} for W512KO-MDE, 0.15 ± 0.03 s^{-1} for W29-MDE, and 0.48 ± 0.28 s^{-1} for W36-MDE. The K_M values are 63 ± 15 μM, 35 ± 40 μM, 26 ± 17 μM, and 8 ± 37 μM for WT-MDE, W512KO-MDE, W29-MDE, and W36-MDE, respectively. Thus the catalytic efficiencies (V_{max}/K_M) for WT-MDE, W512KO-MDE, W29-MDE, and W36-MDE are $2.7 \times 10^3\ M^{-1}s^{-1}$, $2.3 \times 10^3\ M^{-1}s^{-1}$, $5.8 \times 10^3\ M^{-1}s^{-1}$, and $6.0 \times 10^4\ M^{-1}s^{-1}$, respectively.

Fluorescence enhancement

Smooth muscle myosin exhibits an increase in tryptophan fluorescence upon ATP binding (M* · ATP), followed by a further enhanced tryptophan fluorescent state (M** · ADP.P*i*) upon ATP hydrolysis (Fig. 2) (Johnson and Taylor, 1978; Rosenfeld and Taylor, 1984; Woodward et al., 1995; Cremo and Geeves, 1998). We have previously demonstrated that W512, a conserved tryptophan residue located in the relay loop of smooth muscle myosin, undergoes a similar pattern of intrinsic fluorescence enhancement, only to a greater extent, compared to the wild-type molecule (Yengo et al., 2000). Therefore, to test the hypothesis that W512 uniquely contributes to the observed intrinsic fluorescence enhancement upon nucleotide binding and hydrolysis in smooth muscle myosin, we created a mutant construct containing six of the seven tryptophan residues endogenous to the wild-type molecule (at positions 29, 36, 441, 546, 597, and 625), lacking only W512 (which was conservatively replaced with phenylalanine). The percent enhancements and emission maximum of steady-state tryptophan fluorescence of the nucleotide-containing complexes as compared to the nucleotide free (apo) states for each of our MDE constructs are presented in Table 2. WT-MDE has previously been shown to exhibit an intrinsic fluorescence with enhancements of 12.1 ± 0.0% in the presence of ADP and 18.4 ± 0.0% during

TABLE 1 Actin-activated Mg-ATPase activity of wild-type and mutant MDEs

Construct	V_{max} (s^{-1})	K_M (μM)	Catalytic efficiency V_{max}/K_M ($M^{-1}s^{-1}$)
WT-MDE (5)	0.17 ± 0.09	63 ± 15	2.7×10^3
W512 KO-MDE (2)	0.08 ± 0.05	35 ± 40	2.3×10^3
W29-MDE (3)	0.15 ± 0.03	26 ± 17	5.8×10^3
W36-MDE (3)	0.48 ± 0.28	8 ± 37	6.0×10^4

Dependence of steady-state ATPase activity on actin concentration. V_{max} and K_M values (mean ± SD) were calculated by plotting actin-activated ATPase rates as a function of actin concentration and fitting the curves to Michaelis-Menton kinetics. The number of times the experiment was repeated is given in parentheses.

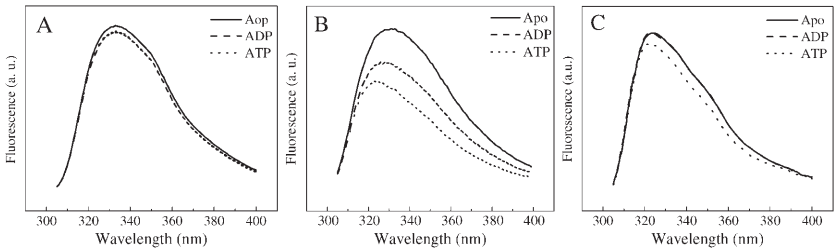

FIGURE 2 Fluorescence emission spectra of W512 KO-MDE, W29-MDE, and W36-MDE. The steady-state fluorescence spectra in the presence of nucleotides are compared to the nucleotide free environment (apo). (*A*) The percent increase in peak fluorescence of W512 KO-MDE in the presence of 200 μM ADP is -3% and in the presence of 2 mM ATP is -6%. (*B*) The percent increase in peak fluorescence of W29-MDE in the presence of 200 μM ADP is -21% and in the presence of 2 mM ATP is -29%. The emission peak wavelength for W29 in the nucleotide-free state showed a 4 nm blue shift in the presence of ADP, and an even greater 5 nm blue shift in the presence of ATP. (*C*) The percent increase in peak fluorescence of W36-MDE in the presence of 200 μM ADP is -3% and in the presence of 2 mM ATP is -8%. The emission maximum of W36 is not sensitive to nucleotide binding.

steady-state hydrolysis of ATP, and W512-MDE has previously been shown to exhibit an intrinsic fluorescence with enhancements of 30.1 ± 2.1% in the presence of ADP and 36.1 ± 1.1% during steady-state hydrolysis of ATP, as compared to the nucleotide-free state, respectively (Yengo et al., 2000). In contrast, the W512 KO-MDE mutant demonstrates a quenching of $-2.9 \pm 1.7\%$ in the presence of ADP, and a further quench to $-5.6 \pm 1.9\%$ during the steady-state hydrolysis of ATP, as compared to the nucleotide free state, respectively (Fig. 2 *A*). In addition, the emission peak maximum of W512 KO-MDE (334 ± 2 nm) is almost identical to that of WT-MDE (336 ± 0 nm) (Yengo et al., 2000). Thus, the decreased fluorescence of W512 KO-MDE indicates that W512 is not the only tryptophan that contributes to the observed changes in intrinsic fluorescence upon nucleotide binding and/or hydrolysis in smooth muscle myosin. Furthermore, the other tryptophan residue(s) that are sensitive to nucleotide binding and/or hydrolysis have an opposing effect (i.e., a decrease of overall intrinsic fluorescence intensity is observed) to that of W512.

We have previously demonstrated that four of the six remaining tryptophans (at positions 441, 546, 597, and 625) are not sensitive to nucleotide binding or hydrolysis, leaving W29 and W36 as candidates for the quench in intrinsic tryptophan fluorescence observed upon nucleotide binding in the W512KO-MDE construct. Residues W29 and W36 are located adjacent to and within the SH3 domain (residues 33–76) at the N-terminus of the molecule. Therefore, we have generated two mutants of smooth muscle myosin in which all the endogenous tryptophans are absent except either W29 or W36. We examined the steady-state fluorescence properties of W29-MDE and W36-MDE in the presence of nucleotides and compared these properties both qualitatively and quantitatively to the nucleotide-free state and to WT-MDE (Table 2, Fig. 2). The emission peak wavelength for W29 in the nucleotide-free state (332 ± 3) was blue-shifted 4 nm in comparison to WT-MDE, showed an additional 4 nm blue shift in the presence of ADP (328 ± 1), and an even greater 5 nm blue shift in the presence of ATP (327 ± 2) (Table 2, Fig. 2 *B*). The emission peak wavelength for W36-MDE (325 ± 2) was blue-shifted 11 nm from WT-MDE, but like WT-MDE, the emission maximum did not change in the presence or absence of nucleotides (Table 2, Fig. 2 *C*). The tryptophan fluorescence of W29-MDE is quenched $-20.7 \pm 6.4\%$ in the presence of ADP and $-28.9 \pm 3.0\%$ in the presence of ATP. In contrast, W36-MDE tryptophan fluorescence is quenched only $-3.4 \pm 2.3\%$ in the presence of ADP and $-7.7 \pm 0.8\%$ in the presence of ATP (Table 2, Fig. 2 *C*).

As seen above, the steady-state response of W29-MDE to nucleotide binding exhibits both a decrease in fluorescence intensity and a blue shift in its emission maximum. The presence of these two characteristics together is paradoxical, since a blue shift is often indicative of a change in conformation resulting in a more hydrophobic environment, whereas a decrease in fluorescence is often indicative of a conformational change resulting in a more hydrophilic

TABLE 2 Tryptophan fluorescence enhancement relative to the nucleotide free state

Nucleotide complex	WT-MDE*	W512-MDE*	W512 KO-MDE	W29-MDE	W36-MDE
Enhancement (%):					
ADP	12.1 ± 0.0	30.1 ± 2.1	−2.9 ± 1.7	−20.7 ± 6.4	−3.4 ± 2.3
ATP	18.4 ± 0.0	36.1 ± 1.1	−5.6 ± 1.9	−28.9 ± 3.0	−7.7 ± 0.8
	n = 5	n = 5	n = 4	n = 5	n = 3
Emission max. (nm):					
Apo	336 ± 0	336 ± 0	334 ± 2	332 ± 3	325 ± 2
ADP	336 ± 0	336 ± 0	334 ± 2	328 ± 1	325 ± 2
ATP	336 ± 0	336 ± 0	334 ± 2	327 ± 2	325 ± 2
	n = 5	*n* = 5	*n* = 4	*n* = 5	*n* = 4

The mean ± SD enhancement in the peak fluorescence intensity of WT-MDE, W512-MDE, W512 KO-MDE, W29-MDE, and W36-MDE-MDE in the presence of ADP or ATP are expressed relative to the nucleotide-free state. The peak emission wavelength ±SD in the absence and presence of nucleotide is also reported.

*Yengo et al. (2000).

environment, around the tryptophan residue. Acrylamide quenching is dependent upon the number of collisions between the tryptophan and acrylamide molecules in the surrounding solvent. Thus the more solvent accessible the tryptophan, the more easily it is quenched by interactions with acrylamide. We examined the solvent exposure of W29 and W36 in different nucleotide states by acrylamide quenching experiments. The Stern-Volmer relationship was used to quantitatively assess the amount of acrylamide quenching (Fig. 3). The Stern-Volmer constant of W36-MDE was not dependent on nucleotide as $K_{SV} = 2.04\ M^{-1}$ in the absence of nucleotide and $K_{SV} = 2.17\ M^{-1}$ in the presence of 2 mM ATP. In contrast, the Stern-Volmer constant of W29-MDE decreased 32% from 6.79 M^{-1} in the absence of nucleotide to 4.63 M^{-1} in the presence of 2 mM ATP. When normalized to the average excited-state lifetime (τ_{avg}) (Fig. 4, Table 3), the dynamic Stern-Volmer constant can be used to calculate the underlying bimolecular quenching constant ($k_q = K_{SV}/\tau_{avg}$), a measure of the collisional rate between the fluorophore and solvent quencher molecules. The bimolecular quenching constants were determined to be $8.0 \times 10^8\ M^{-1}s^{-1}$ and $4.8 \times 10^8\ M^{-1}s^{-1}$ for W29-MDE in the absence and presence of ATP, respectively, and $2.8 \times 10^8\ M^{-1}s^{-1}$ and $2.6 \times 10^8\ M^{-1}s^{-1}$ for W36-MDE in the absence and presence of ATP, respectively (Table 3). These data are consistent with the conclusion that W29 becomes less accessible to solvent in the presence of ATP, whereas the accessibility of W36 is largely unchanged. Thus, in agreement with the observed steady-state fluorescence emission maxima data, the acrylamide quenching results suggest that W29 is in a less polar, less solvent-exposed environment in the nucleotide states that bind weakly to actin (M·ATP and M·ADP·P*i*) relative to the strongly bound nucleotide free state of the ATPase cycle.

Proteins that display a blue-shifted emission spectrum are expected to have higher steady-state fluorescence intensities or longer lifetimes based on the usual increase in quantum yield when a fluorophore is placed in a less polar environment. In addition to the steady-state fluorescence characterizations, we also determined the quantum yields of W29 and W36 in the presence and absence of nucleotide by lifetime analysis (τ_{avg}/τ_0), where the intrinsic lifetime (τ_0) is assumed to be 16 ns (Lakowicz, 1983). The quantum yield of the excited state of W29 is slightly greater in the nucleotide-free state (0.15) than in the presence of either 200 μM ADP or 2 mM ATP (0.12). However, upon ATP binding the difference in the excited-state quantum yield of W29 (20%) is smaller than the observed decrease in steady-state fluorescence intensity (29%), suggesting that the observed quench in the presence of ATP is a consequence of both ground-state and excited-state phenomena. Conversely, the quantum yield of the excited state of W36 is unchanging regardless of the nucleotide state, at 0.17 in the absence of ATP and 0.18 in the presence of 2 mM ATP. Therefore, the

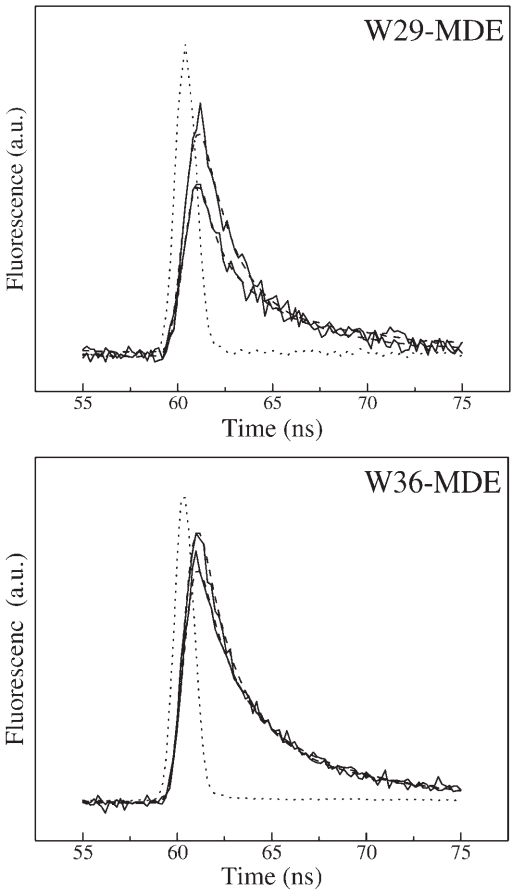

FIGURE 4 Time-resolved fluorescence decays of W29-MDE and W36-MDE in the absence (apo) and presence of 2 mM ATP. Each trace represents the average of eight data sets. The instrument response function (*dotted line*) is the laser pulse profile measured from a scattering solution in the sample cuvette. Dashed lines are the best fit to a two-exponential decay. W29-MDE demonstrated a quench in fluorescence intensity upon ATP addition, whereas W36-MDE did not significantly change in fluorescence intensity upon nucleotide addition. The measured average lifetimes are presented in Table 3.

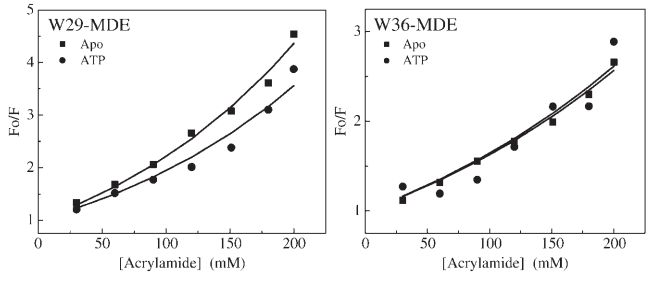

FIGURE 3 Acrylamide quenching of W36-MDE and W29-MDE in the presence of 2 mM ATP or in the absence of nucleotide (apo). The relative change in fluorescence (F_0/F) is plotted as a function of increasing acrylamide (mM), and the data points are fit to the Stern-Volmer relationship ($F_0/F = (1 + K_{SV}\ [Q])\exp V[Q]$, where K_{SV} is the dynamic quenching constant and V is the static quenching constant previously determined to be 3.0 M^{-1} (Yengo et al., 2000)).

TABLE 3 Spectroscopic data

Nucleotide complex	Lifetime τ_{avg} (ns)	Quantum yield Φ	Stern-Volmer constant K_{SV} (M^{-1})	Bimolecular quenching constant k_q ($M^{-1}s^{-1}$)
W29-MDE				
Apo	2.4	0.15	6.79	8.0×10^8
ADP	2.0	0.12	n.d.	n.d.
ATP	2.0	0.12	4.63	4.8×10^8
W36-MDE				
Apo	2.7	0.17	2.04	2.8×10^8
ATP	2.9	0.18	2.17	2.6×10^8

The time-resolved quantum yield (Φ), Stern-Volmer constant (K_{SV}), and bimolecular quenching constants (k_q) are reported for W29-MDE and W36-MDE-MDE in the presence of ADP, ATP, or in the nucleotide-free state. Weighted average fluorescence lifetimes (τ_{avg}) are determined by the equation $[\tau_1 \times A_1/(A_1 + A_2)] + [\tau_2 \times A_2/(A_1 + A_2)]$. The quantum yield is reported relative to the natural tryptophan lifetime (16 ns). The bimolecular quenching constant (k_q) is given by K_{sv}/τ_{avg}. Standard errors in the fitted parameters were <25% of the values given. Parameters deduced from experimental runs ($n = 3$–4) agreed within 15% of the values given.

observed quenching of W36 is most likely due to strictly ground-state phenomena.

DISCUSSION

Much of the kinetic information about the first two steps of the skeletal and smooth muscle myosin II ATPase cycle, ATP binding and hydrolysis, has been elucidated by following changes in the intrinsic tryptophan fluorescence, which shows an enhancement upon ATP binding and a further enhancement upon ATP hydrolysis (Johnson and Taylor, 1978; Rosenfeld and Taylor, 1984; Woodward et al., 1995; Cremo and Geeves, 1998). However, little is known about the structural basis underlying these changes in intrinsic tryptophan fluorescence. To investigate such structural changes, one must first identify the tryptophans responsible for the observed intrinsic fluorescence signals. We have previously demonstrated that W512 is one of the tryptophan residues responsible for changes in intrinsic fluorescence during the ATPase cycle of smooth muscle myosin (Yengo et al., 2000). In this study, we have investigated whether tryptophan 512 is uniquely sensitive to nucleotide binding and hydrolysis in smooth muscle myosin. The W512 KO-MDE demonstrated a small quench in tryptophan fluorescence in the presence of nucleotide, providing evidence that W512 is not uniquely sensitive in smooth muscle myosin. Given that we have already shown that the conserved tryptophans W441 and W597 (Yengo et al., 2000), as well as the isoform specific tryptophans W546 and W625 (Yengo et al., 1998), are not sensitive to nucleotide binding and hydrolysis in smooth muscle myosin,W29 and W36, both unique to smooth muscle myosin, are likely candidates for the changes in intrinsic fluorescence observed upon nucleotide binding in W512 KO-MDE.

Functional properties of WT-, W512 KO-, W29-, and W36-MDE

Michaelis-Menton kinetic constants for the actin-activated ATPase activity of WT-MDE were previously reported (Yengo et al., 2000) and repeated for this study. The W512 KO-MDE and W29-MDE constructs show reduced values of V_{max} relative to the WT-MDE molecule, whereas W36-MDE shows an increased value of V_{max} relative to WT-MDE (Table 1). However, all four constructs (WT-MDE, W512 KO-MDE, W29-MDE, and W36-MDE) demonstrate a significant actin-activated ATPase activity, and all three mutants show decreased K_M values relative to WT-MDE. Although the V_{max} and K_M values vary between the constructs (Table 1), the catalytic efficiencies of WT-MDE, W512 KO-MDE, and W29-MDE are comparable, whereas the W36-MDE is ~10-fold more efficient than even the WT-MDE. Likewise, P*i* release is the rate-limiting step of the ATPase for all of the smooth muscle myosin constructs used in our studies (manuscript submitted). Thus, although the mutant proteins may have small variations in rate or equilibrium constants between specific states of the ATPase cycle (M. van Duffelen, L. R. Chrin, and C. L. Berger, unpublished), the overall catalytic cycle is quite similar for all the constructs of smooth muscle myosin used in this study.

Contribution of W29 and W36 to the overall intrinsic fluorescence changes in smooth muscle myosin

As demonstrated previously (Yengo et al., 2000) and in this work, W512 is one of the major contributors to changes in intrinsic fluorescence during the ATPase cycle of smooth muscle myosin. The corresponding residues in the relay loops of myosin II from skeletal muscle (W510, (Park and Burghardt, 2000)) and the slime mold *D. discoideum* (W501, (Batra and Manstein, 1999; Málnási-Csizmadia et al., 2000)) have also been shown to be the primary contributors to the nucleotide-dependent changes in intrinsic tryptophan fluorescence in these isoforms, and in the case of myosin II from *D. discoideum*, W501 has been shown to be the only endogenous tryptophan in the motor domain that is sensitive to nucleotide binding (Málnási-Csizmadia et al., 2000). Likewise, W510 has been proposed to be the sole contributor to the nucleotide-dependent changes in tryptophan fluorescence for skeletal muscle myosin (Park and Burghardt, 2000). However, when two tryptophans are introduced into the *D. discoideum* motor domain at positions 113 and 131, which correspond to those uniquely present in vertebrate skeletal muscle myosin, these residues also contribute to the observed nucleotide dependent changes in intrinsic fluorescence for that isoform, albeit to a lesser extent than W510 (Kovács et al., 2002). Thus, whereas the conserved tryptophan residue at position 512 of the relay loop in smooth muscle myosin appears to be a major contributor to

nucleotide-dependent changes in intrinsic fluorescence as in all isoforms of myosin, isoform-specific differences also exist resulting from the presence of unique nonconserved tryptophans in other conformationally sensitive regions of the myosin molecule. Such isoform-specific tryptophan residues may play a role in the response of smooth muscle myosin in nucleotide binding and hydrolysis, and provide new information regarding structural changes associated with specific steps of the ATPase cycle.

Unlike W512-MDE, which shows a large increase in intrinsic fluorescence in response to both ADP (30%) and ATP (36%) when compared to the nucleotide free state (Yengo et al., 2000), W512 KO-MDE shows a small decrease in intrinsic fluorescence in response to both ADP (−3%) and ATP (−6%) when compared to the nucleotide free state. This provides evidence for the existence of intrinsic fluorescence contributions from the previously uninvestigated tryptophan residues, W36 and W29 in smooth muscle myosin, given that W441, W546, W597, and W625 have all been previously shown to be insensitive to nucleotide binding (Yengo et al., 2000). We found that W36-MDE also shows a small decrease in intrinsic fluorescence in response to both ADP (−3%) and ATP (−8%) when compared to the nucleotide free state. Thus, given these small changes, in the presence of the other six endogenous tryptophans, W36 is unlikely to contribute significantly to the observed nucleotide-dependent changes in intrinsic fluorescence of the wild-type molecule. However, W29-MDE exhibits a large quench in intrinsic fluorescence in response to both ADP (−21%) and ATP (−29%), and therefore is likely to contribute substantially to the nucleotide-dependent intrinsic fluorescence changes observed in both the WT- and W512 KO-MDE molecules. Thus, the intrinsic fluorescence of tryptophans W512, W29, and W36 are all sensitive to nucleotide binding in smooth muscle myosin.

Structural basis for nucleotide-dependent changes in W29 and W36 intrinsic fluorescence

The decrease in fluorescence intensity is accompanied by a spectral blue shift upon nucleotide binding in W29-MDE (Table 2, Fig. 2). A spectral blue shift is often indicative of a conformational change to a more hydrophobic environment, whereas a decrease in fluorescence intensity is often indicative of a conformational change to a more hydrophilic environment. This paradox can be resolved by collisional quenching experiments, which are a measure of the solvent accessibility of the fluorophore. The Stern-Volmer and bimolecular quenching constants of W29-MDE both decrease upon ATP binding as compared to the apo state (Table 3, Fig. 3), consistent with the observed blue shift of W29 fluorescence upon nucleotide binding. These results indicate a decrease in solvent exposure of W29, and thus a decrease in solvent relaxation of the tryptophan residue in the more buried state. There is also a small decrease in fluorescence intensity without a spectra shift upon ATP binding for W36 (Table 2, Fig. 2). The Stern-Volmer constants and the bimolecular quenching constants are not nucleotide-dependent (Table 3, Fig. 3), therefore the solvent accessibility of W36 does not change upon ATP binding. The relatively low Stern-Volmer and bimolecular quenching constants, as well as the relatively blue-shifted emission maxima, suggest that both W29 and W36 are predominantly buried in the smooth muscle myosin molecule. Analysis of the smooth muscle myosin MDE crystal structures in the presence of AlF_4^- and BeF_x show that the W29 and W36 indole rings are 39% and 1.5% exposed to the solvent, respectively. Interestingly, the B-factor for the W29 residue is relatively high, suggesting heterogeneity in the position of this side chain despite being largely buried in the protein structure, whereas the B-factor for the W36 residue is relatively low as expected. These results are consistent with our observations that both tryptophan residues are not easily quenched by solvent interactions, with W36 being more protected than W29. The increased dynamics of the W29 side chain may reflect the ability of this region of the molecule, a loosely structured loop, to adopt multiple conformations. Clearly, our data strongly support such a possibility.

Decreases in steady-state fluorescence emission can arise from a combination of ground- and excited-state quenching mechanisms, whereas time-resolved emission decays are sensitive only to excited-state relaxation phenomena. Therefore, we also measured the fluorescence lifetimes of both W29 and W36 (Table 3). Consistent with the steady-state observations, the number of excited-state tryptophans decreases slightly for W36 and decreases substantially for W29, as indicated by the peak intensity of the fluorescence emission decay profile (Fig. 4). W36-MDE time-resolved fluorescence emission decays are not nucleotide-dependent (Table 3), indicating that the fluorescence of W36 is quenched predominantly by a ground-state mechanism upon nucleotide binding. In contrast, time-resolved quantum yield determinations of W29 show a 20% decrease upon nucleotide binding, but no difference is observed whether the nucleotide is ADP or ATP (Table 3). This result is consistent with an excited-state mechanism responsible for the steady-state fluorescence quench observed upon nucleotide binding (~20%). The additional ~10% decrease in intrinsic fluorescence observed under steady-state conditions upon the binding of ATP relative to ADP by W29-MDE appears to involve an additional ground-state quenching mechanism as there is no observed difference in the excited-state quantum yield. The extension of this is that the ATP binding event alters the W29 ground state so that it is less excitable than in the presence of ADP.

The indole ring of tryptophan has the potential to be quenched by neighboring residues, and the degree of quenching is dependent on both the orientation and distance

between the two side chains. Within the sequence surrounding the W29 tryptophan in both the ADP · AlF_4^- (Fig. 5) and ADP · BeF_x crystal structures (Dominguez et al., 1998), K32 is a charged residue within 4–5 Å of the face of the indole ring of W29. Therefore, one possibility is that the observed quench in W29 fluorescence may be due to the interaction of K32 with the pi electrons of the indole ring of W29. Thus, W29 and K32 may alter their orientation and molecular distance with respect to one another, resulting in different levels of quenching in different states of the ATPase cycle. Alternatively, other residues may be involved since W29 is located in a conformationally sensitive loop of the smooth muscle myosin molecule. It will be interesting to examine other smooth muscle myosin structures as they become available for possible interactions between W29 and other amino acid side chains such as K32.

Functional implications for nucleotide-dependent changes in W29 and W36 intrinsic fluorescence

W36 is located within the smooth muscle myosin N-terminal SH3 domain, whereas W29 is located in an adjacent loosely structured loop. The SH3 domain is an antiparallel β-barrel in the N-terminus comprising residues 33–76. One of the first indications of nucleotide-dependent structural changes in this region of the molecule for either skeletal or smooth muscle myosin was the observation that R23 in skeletal S1 is cleaved by trypsin in the presence of ATP but not in the absence of ATP (Pinter et al., 1986). Subsequently, cryoelectron microscopy has shown that the helix in the N-terminal region of smooth muscle myosin (residues 21–31) is altered in the ADP bound state as compared to the apo state, and has been associated with movement of the lever arm upon ADP release (Whittaker et al., 1995). Differences have also been observed in the structure of the SH3 domain between different isoforms of myosin. X-ray crystallography studies found that the first 33 amino acids of the N-terminal domain of the smooth muscle MDE-AlF_4^- structure (Dominguez et al., 1998), containing W29, fold differently than either skeletal S1 (Rayment et al., 1993) or the *D. discoideum* motor domain (Fisher et al., 1995). These structural differences at least in part reflect sequence variations between isoforms as the N-terminus of myosin is not highly conserved. However, such structural differences may also have important functional implications. For example, in the skeletal muscle myosin structure (Rayment et al., 1993), the N-terminal residues of the myosin heavy chain interact with the ELC, which may help stabilize the position of the lever arm in the postpower stroke state. Conversely, the ELC makes contacts with the 25K-50K loop near the active site rather than the N-terminal residues of the ADP · AlF_4^- smooth muscle myosin structure, thought to be in a prepower stroke state (Dominguez et al., 1998). Furthermore, the N-terminal residues are disordered in a structure of smooth muscle myosin lacking the lever arm and ELC, but form a loosely structured loop in the presence of a truncated lever arm including the ELC (Dominguez et al., 1998). Our results directly demonstrate, in solution, the conformational sensitivity of this region of the smooth muscle myosin molecule. Thus, evidence is growing for the functional significance of conformational changes in the N-terminal domain of myosin, which may stabilize interactions of the myosin heavy chain with the ELC, and therefore different positions of the lever arm. The unique spectroscopic signal of W29 upon nucleotide binding should provide a powerful tool for further elucidating structural changes in the N-terminus of smooth muscle myosin associated with specific states of the ATPase cycle.

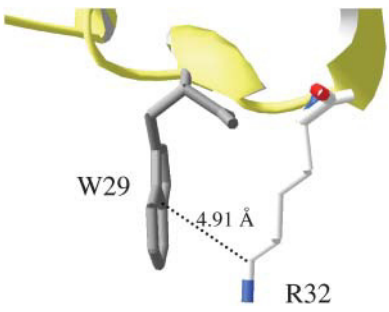

FIGURE 5 View of the location of W29 in the ADP · AlF_4^- crystal structure of the smooth muscle myosin MDE construct with the myosin heavy chain colored yellow. The W29 and R32 residues are shown in a stick format, with a distance of 4.91 Å between them (Dominguez et al., 1998).

We thank Christopher M. Yengo for the W512-MDE and Null-MDE constructs and Kathleen M. Trybus for the WT-MDE construct. We thank Donald P. Gaffney for helpful discussions and Scott Barbick for excellent technical assistance. We also thank Mark A. Rould for the solvent accessibility analysis of the tryptophan residues W29 and W36.

This work was supported by a grant to C.L.B. from the National Institutes of Health (HL63798).

REFERENCES

Bagshaw, C. R., J. F. Eccleston, F. Eckstein, R. S. Goody, H. Gutfreund, and D. R. Trentham. 1974. The magnesium ion-dependent adenosine triphosphatase of myosin. *Biochem. J.* 141:351–364.

Bagshaw, C. R., and D. R. Trentham. 1974. The characterization of myosin-product complexes and of product-release steps during the magnesium ion-dependent adenosine triphosphatase reaction. *Biochem. J.* 141:331–349.

Batra, R., and D. J. Manstein. 1999. Functional characterization of *Dictyostelium* myosin II with conserved tryptophanyl residue 501 mutated to tyrosine. *Biol. Chem.* 380:1017–1023.

Cooke, R. 1999. Myosin structure: Does the tail wag the dog? *Curr. Biol.* 9:R773–R775.

Cremo, C. R., and M. A. Geeves. 1998. Interaction of actin and ADP with the head domain of smooth muscle myosin: implications for strain-dependent ADP release in smooth muscle. *Biochemistry.* 37:1969–1978.

De la Cruz, E. M., H. L. Sweeney, and E. M. Ostap. 2000. ADP inhibition of myosin V ATPase activity. *Biophys. J.* 79:1524–1529.

Dominguez, R., Y. Freyzon, K. M. Trybus, and C. Cohen. 1998. Crystal structure of a vertebrate smooth muscle myosin motor domain and its

complex with the essential light chain: visualization of the pre-power stroke state. *Cell.* 94:559–571.

Eftink, M. R., and C. A. Ghiron. 1976. Exposure of tryptophanyl residues in proteins. Quantitative determination by fluorescence quenching studies. *Biochemistry.* 15:672–680.

Fisher, A. J., C. A. Smith, J. A. Thoden, R. Smith, K. Sutoh, H. M. Holden, and I. Rayment. 1995. X-ray structures of the myosin motor domain of *Dictyostellium discoideum* complexed with MgADP:BeFx and MgADP:AlF_4^-. *Biochemistry.* 34:8960–8972.

Furch, M., M. A. Geeves, and D. J. Manstein. 1998. Modulation of actin affinity and actomyosin adenosine triphosphatase by charge changes in the myosin motor domain. *Biochemistry.* 37:6317–6326.

Geeves, M. A., and K. C. Holmes. 1999. Structural mechanism of muscle contraction. *Annu. Rev. Biochem.* 68:687–728.

Houdusse, A., and H. L. Sweeney. 2001. Myosin motors: missing structures and hidden springs. *Curr. Opin. Struct. Biol.* 11:182–194.

Huxley, A. F. 1969. The mechanism of muscular contraction. *Science.* 164:1356–1366.

Huxley, A. F., and J. E. Hansen. 1954. Changes in the cross-striations of muscle during contraction and stretch and their structural interpretation. *Nature.* 173:973–976.

Huxley, A. F., and R. Niedergerke. 1954. Structural changes in muscle during contraction. Interference microscopy of living muscle fibers. *Nature.* 173:971–973.

Johnson, K. A., and E. W. Taylor. 1978. Intermediate states of subfragment 1 and actosubfragment 1 ATPase: reevaluation of the mechanism. *Biochemistry.* 17:3432–3442.

Kovács, M., A. Málnási-Csizmadia, R. J. Woolley, and C. R. Bagshaw. 2002. Analysis of nucleotide binding to *Dictyostelium* myosin II motor domains containing a single tryptophan near the active site. *J. Biol. Chem.* 277:28459–28467.

Lakowicz, J. R. 1983. Principles of Fluorescence Spectroscopy. Plenum Press, New York.

Lymn, R. W., and E. W. Taylor. 1971. Mechanism of adenosine triphosphate hydrolysis by actomyosin. *Biochemistry.* 10:4617–4624.

Málnási-Csizmadia, A., R. J. Woolley, and C. R. Bagshaw. 2000. Resolution of conformational states of *Dictyostelium* myosin II motor domain using tryptophan (W501) mutants: implications for the open-closed transition identified by crystallography. *Biochemistry.* 39:16135–16146.

Marston, S. B., and E. W. Taylor. 1980. Comparison of the myosin and actomyosin ATPase mechanisms of the four types of vertebrate muscles. *J. Mol. Biol.* 139:573–600.

Park, S., K. Ajtai, and T. P. Burghardt. 1997. Mechanism of coupling free energy in ATPase to the myosin active site. *Biochemistry.* 36:3368–3372.

Park, S., and T. P. Burghardt. 2000. Isolating and localizing ATP-sensitive tryptophan emission in skeletal myosin subfragment 1. *Biochemistry.* 39:11732–11741.

Pinter, K., R. C. Lu, and L. Szilagyi. 1986. Thermal stability of myosin subfragment-1 decreases upon tryptic digestion in the presence of nucleotides. *FEBS Lett.* 200:221–225.

Rayment, I., W. R. Rypniewski, K. Schmidt-Bäse, R. Smith, D. R. Tomchick, M. M. Benning, D. A. Winklemann, G. Wesenberg, and H. M. Holden. 1993. Three-dimensional structure of myosin subfragment-1: a molecular motor. *Science.* 261:50–58.

Rosenfeld, S. S., and E. W. Taylor. 1984. The ATPase mechanism of skeletal and smooth muscle acto-subfragment 1. *J. Biol. Chem.* 259:11908–11919.

Whittaker, M., E. M. Wilson-Kubalek, J. E. Smith, L. Faust, R. A. Milligan, and H. L. Sweeney. 1995. A 35-Å movement of smooth muscle myosin on ADP release. *Nature.* 378:748–751.

Woodward, S. K. A., M. A. Geeves, and D. J. Manstein. 1995. Kinetic characterization of the catalytic domain of *Dictyostelium discoideum* myosin. *Biochemistry.* 34:16056–16064.

Yengo, C. M., L. R. Chrin, A. S. Rovner, and C. L. Berger. 2000. Tryptophan 512 is sensitive to conformational changes in the rigid relay loop of smooth muscle myosin during the MgATPase cycle. *J. Biol. Chem.* 275:25481–25487.

Yengo, C. M., P. M. Fagnant, L. R. Chrin, A. S. Rovner, and C. L. Berger. 1998. Smooth muscle myosin mutants containing a single tryptophan reveal molecular interactions at the actin-binding interface. *Proc. Natl. Acad. Sci. USA.* 95:12944–12949.